

Study of γ -irradiated Polymer Electrolyte for Zn Rechargeable Nanostructured Galvanic Cells by SAXS/DSC/WAXD method

A. Turković · P. Dubček · K. Juraić ·
M. Rakić · S. Bernstorff

Received: 11 November 2010 / Accepted: 11 February 2011
© Springer Science+Business Media, LLC 2011

Abstract $(\text{PEO})_8\text{ZnCl}_2$ polymer electrolytes and nanocomposites were prepared using PEO γ -irradiated with a dose of 529 kGy. The effect of γ -radiation from a Co-60 source were studied by small-angle X-ray scattering simultaneously recorded with differential scanning calorimetry and wide-angle X-ray diffraction at the synchrotron ELETTRA. The abovementioned treatment largely enhanced the conductivity of the polymer electrolyte. A room temperature conductivity increase by up to two orders of magnitude was achieved by Turković et al. (J Electrochem Soc 154(6):A554, 2007).

Keywords Polymer electrolytes · Nanocomposites · SAXS/DSC/WAXD

1 Introduction

Understanding the structure of new materials on the mesoscopic scale (2–50 nm), such as clusters, aggregates and

nano-sized materials, requires suitable experimental techniques. Electromagnetic radiation can be used to obtain information about materials whose dimensions are on the same order of magnitude as the radiation wavelength. Scattering of X-rays is caused by differences in electron density. Since the larger the diffraction angle the smaller the length scale probed, wide angle X-ray diffraction (WAXD) is used to determine the crystal structure on the atomic length scale while small-angle X-ray scattering (SAXS) is used to explore the microstructure on the nanometer scale.

SAXS experiments are suitable to determine the structure of a nanocomposite polymer electrolyte. The solid electrolyte poly(ethylene oxide) (PEO) is one of the most extensively studied systems due to its relatively low melting point and glass transition temperature, T_g , its ability to play host to a variety of metal salt systems in a range of concentrations; and, recently, it has been shown to be a material with the smallest ever polymer crystals prepared [1]. Polymeric complexes of $(\text{PEO})_n$ with ZnCl_2 have been used due to their stability and very high conductivity [2, 3]. We have observed that the ionic conductivity at room temperature is up to two-times larger compared to that above the phase transition temperature of 65 °C [4]. Our research was aimed at the optimizations of the electrolyte properties [4] as these materials are attractive as electrolytes for second generation polymer-based rechargeable batteries [5, 6] or other types of electronic devices.

The aim of the present investigation was to study the temperature behavior of the γ -irradiated $(\text{PEO})_8\text{ZnCl}_2$ electrolyte by simultaneous SAXS/WAXD/DSC measurements. This structural investigation will provide an answer to questions about the nano-size behavior through the superionic phase transition, which occurs at ~ 65 °C.

A. Turković (✉) · P. Dubček · K. Juraić
Ruđer Bošković Institute, P.O. Box 180, HR-10002 Zagreb,
Croatia
e-mail: turkovic@irb.hr

P. Dubček
e-mail: dubcek@irb.hr

K. Juraić
e-mail: kjuraic@irb.hr

M. Rakić
Institute for Physics, Bijenička 46, 10000 Zagreb, Croatia
e-mail: mrakic@irb.hr

S. Bernstorff
Sincrotrone Trieste, SS 14 km 163, 5 Basovizza,
34149 Trieste, Italy
e-mail: bernstorff@elettra.trieste.it

2 Experimental

The polymer-salt complex was prepared by dissolving ZnCl₂ (Merck) and poly(ethylene oxide) (laboratory reagent, BDH Chemicals, Ltd., Poole, England, Polyox WSR-301, MW = 4 × 10⁶, Prod 29740) in 50% ethanol-water solution in stoichiometric proportions [4]. Prior to the synthesis of the polymer-salt electrolyte, the powdered PEO was irradiated by a cobalt-60 source with a dose of 529 kGy.

Simultaneous SAXS/WAXD/DSC measurements were performed at the Austrian SAXS beamline at the synchrotron ELETTRA, Trieste [7]. A photon energy of 8 keV was used; and, the size of the incident photon beam on the sample was 0.1 × 5 mm² (h × w). For each sample, SAXS and WAXD patterns were measured simultaneously in transmission using two 1D single photon counting gas detectors. The SAXS detector was mounted at a sample-to-detector distance of 1.75 m, corresponding to a q-range of 0.0007–0.032 nm. The WAXD detector was mounted to cover a d-spacing range of 0.32–0.94 nm. The scattering wave vector, s is given by $s = 2\sin\theta/\lambda = q/2\pi$, where 2θ is the scattering angle and $\lambda = 0.154$ nm the used wavelength. The method of interpreting the SAXS scattering data is based on the analysis of the scattering curve, which shows the dependence of the scattering intensity, I , on the scattering wave vector s .

The in-line micro-calorimeter built by the group of Michel Ollivon (CNRS, Paris, France) [8] was used to measure simultaneously SAXS/WAXD and high sensitivity DSC from the same sample. The DSC phase transition temperature was determined at the intersection of the tangent to the peak and the baseline.

SAXS is observed when electron density inhomogeneities of nano-sized objects exist in the sample. If identical grains of constant electron density, ρ , are imbedded in a medium of constant ρ_0 , only the difference $\Delta\rho = (\rho - \rho_0)$ will be relevant for scattering. If grains are distanced from each other widely enough, it is assumed that they contribute independently to the scattered intensity. The central peak arises from all added secondary waves in phase at $s = 0$. The amplitude is proportional to $\Delta\rho$ as only the contrast to the surrounding medium is effective. For the central part of the scattering curve, the universal Guinier approximation for all types of scattering objects/grains is valid [9–13] and the scattering intensity is given by Eq. 1 where R_g is the gyration radius, which is the average square distance from the centre of masses within the particles. The average grain radius R , which will be used in our discussion, is derived from R_g applying transformation for a spherical shape of nano-grains.

$$I(s) = (\Delta\rho)^2 \exp(-R_g^2 s^{2/3}) \quad (1)$$

For WAXD the diameter, D , of the nanocrystalline grains is obtained by the Debye–Scherrer Eq. 2 where λ is the wavelength of the incident X-ray beam and β is the full width at half maximum of the WAXD line.

$$D = \frac{0.9 \cdot \lambda}{\beta \cdot \cos(\theta)} \quad (2)$$

3 Results and Discussion

Figure 1 shows the results from the DSC, SAXS and WAXD measurements on the polymer electrolyte (PEO)₈ZnCl₂ nanocomposite. The measurements were performed simultaneously at the SAXS-beamline of ELETTRA. The evolution of the average radii of the grain sizes (R) obtained by applying Eq. 1 is compared to the corresponding DSC and WAXD spectra behaviour. In the heating cycle, the superionic phase transition can be seen as a sudden drop of the nano-grain sizes at the phase transition temperature. In the cooling cycle, a hysteresis can be seen as the phase transition occurs at lower temperature. The endothermic and exothermic peaks found in DSC during the same temperature cycle are in agreement with the sudden changes in the average nano-grain sizes as obtained from the SAXS measurements and intensity drops in the lines in the WAXD spectra.

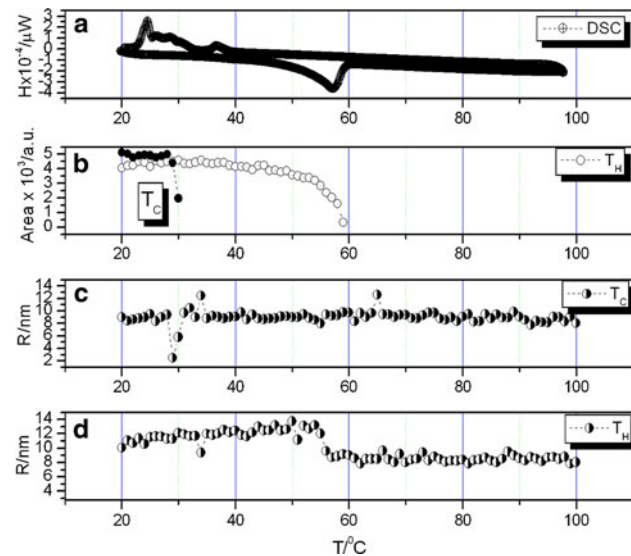


Fig. 1 DSC, WAXD and SAXS results for γ -irradiated (dose 529 kGy) polyelectrolyte (PEO)₈ZnCl₂ from 20 to 100 °C at a heating rate of 1 °C/min; **a** DSC heating and cooling cycle, **b** evolution of the intensity of the strong WAXD line at $2\theta = 19.21$ (denoted with T_H and T_C), **c** average grain radius (R) in the SAXS cooling cycle (denoted with T_C) and **d** R in the SAXS heating cycle (denoted with T_H)

In the heating cycle (rate = 1 °C/min) for the SAXS experiment there are two trends: 1. an increase in the grain size up to 54 °C and 2. a sudden drop at this phase transition temperature. The average grain radius as obtained from Eq. 1 varies from 10 to 13 nm in the region below the phase transition temperature and then from 9 to 8 nm in the highly conductive phase of the polymer electrolyte (54–100 °C). The DSC curve shows the start of the endothermic peak at 51 °C (heating cycle). In the SAXS data, the cooling cycle shows the start of the phase transition at 31 °C; and, the change of the grain sizes is in the range 8.7–8.8 nm for the entire temperature range (100–20 °C). The WAXD spectra show an intensity drop at 59 °C; and, in the cooling cycle the temperature at which recrystallization starts is 30 °C.

In SAXS measurements for repeated heating cycles, the second run (again at 1 °C/min, Fig. 2) results in changes of the grain sizes from 7.9 to 9.1 nm below the phase transition temperature of 52 °C and 7.3–8.0 nm in the highly conductive superionic phase (52–100 °C). The third run (Fig. 3, 3 °C/min) registers changes from 7.8 to 9.0 nm; and, for the fourth run (Fig. 4, 5 °C/min), the grain sizes change from 7.7 to 9.0 nm. In the second run cooling cycle (Fig. 2, 1 °C/min), SAXS results in an almost constant grain size of 7.8 nm for the entire temperature range, 100–20 °C; the third run (Fig. 3, 3 °C/min) registers changes from 8.5 to 9.0 nm; and, during the forth run (Fig. 4, 5 °C/min), the grain sizes vary from 7.2 to 8.1 nm. We can generally conclude that in the heating–cooling cycles SAXS gives an average grain size of 7.2–13 nm for all four runs. In a lamellar picture of PEO [14, 15] these grain sizes would correspond to lamellae LP2 with no

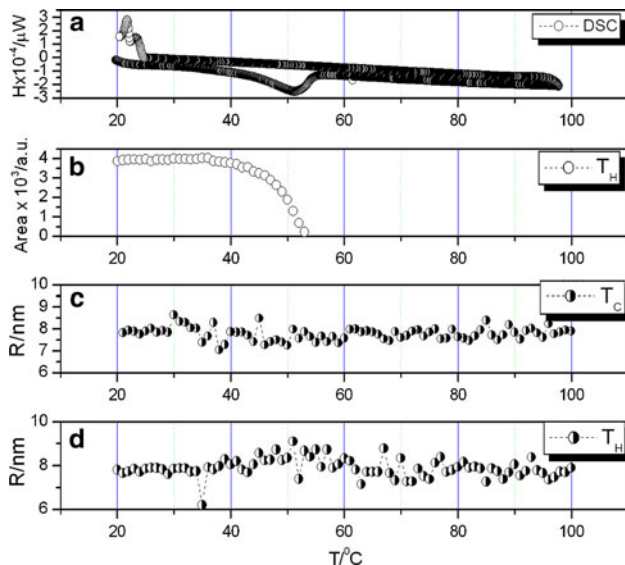


Fig. 2 DSC, WAXD and SAXS results for γ -irradiated polyelectrolyte (PEO)₈ZnCl₂ (heating rate 1 °C/min, second run)

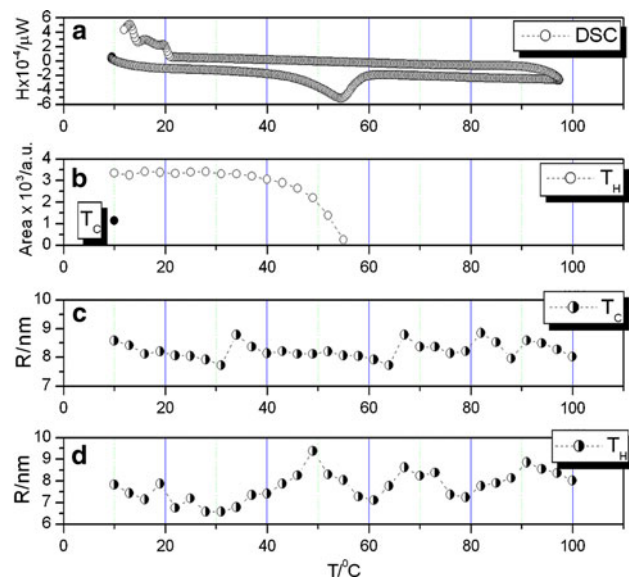


Fig. 3 DSC, WAXD and SAXS results for γ -irradiated polyelectrolyte (PEO)₈ZnCl₂ from 20 to 100 °C at a heating rate of 3 °C/min

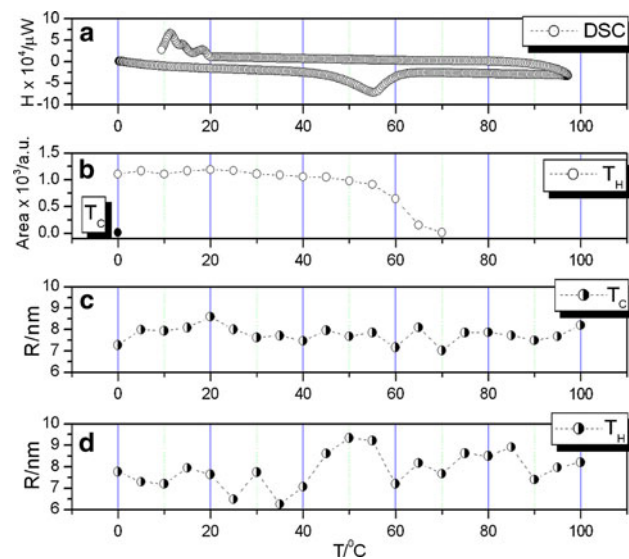


Fig. 4 DSC, WAXD and SAXS results for γ -irradiated polyelectrolyte (PEO)₈ZnCl₂ from 20 to 100 °C at a heating rate of 5 °C/min

integrally folded chains [16, 17] when combined with salt ZnCl₂. The DSC spectra for the rates of 1 °C/min, again 1, 3 and 5 °C/min show that the phase transition temperatures, which are determined at the beginning of the peak in the heating cycle, are 51, 45, 45 and 47 °C, respectively. These temperatures are the melting temperature of the PEO crystallites i.e. “spherulites” [18–20]. In the case of the nanocomposite polymer electrolyte; i.e., the combined forms of PEO and ZnCl₂, ZnCl₂ influences the melting temperature. Both, the SAXS and DSC data show a hysteresis, i.e. much lower phase transition temperatures than 65 °C in the cooling cycle. The DSC curve in the cooling

cycles 1, 1, 3 and 5 °C/min show phase transition temperatures of 38, 25, 21 and 20 °C, respectively.

The WAXD recordings were done simultaneously with the SAXS and DSC measurements. Above the phase transition temperature the WAXD spectra record the amorphous phase of the polymer electrolyte. The most intensive lines in WAXD, which are attributed to combined PEO/ZnCl₂ crystallites, disappear at 59, 53, 55 and 69 °C for heating rates of 1, 1, 3 and 5 °C/min, respectively. However, lines of lower intensity representing the PEO “spherulites” disappear at somewhat lower temperatures. In the cooling cycle, the strongest WAXD lines reappear at 30, 20, 10 and 0°C for cooling rates of 1, 1, 3 and 5°C/min, respectively; and, the lines of lower intensity reappear at lower temperatures. During the heating and cooling cycles, the WAXD data give information about the lateral domain sizes or “spherulites.” The radius of nanocrystallites from Eq. 2 ranges from 7.7 to 1.2 nm in all heating–cooling cycles. The WAXD results for all heating and cooling rates are, together with the SAXS and DSC data, summarized in Table 1. The different hysteresis at the phase transition temperatures for different heating and cooling rates for all the SAXS, WAXD and DSC results are evident. This demonstrates the importance of using the same experimental conditions when comparing literature results. Also, comparing our results from the employed three measurement methods, the obtained differences in the phase transition temperatures are obvious. The best agreement between the phase transition temperatures as obtained by SAXS, WAXD and DSC is achieved during the first cycle with a heating–cooling rate of 1 °C/min, which suggests that

even slower rates, such as 0.5 °C/min [21], might lead to a better agreement between the results of these simultaneously employed measurement methods.

The combination of the three methods, SAXS, WAXD and DSC, reveals the nature of the physical transformation of the polymer electrolyte into a super ionic conductor. The nanocomposite partly crystalline and partly amorphous polymer matrix transforms into an amorphous highly conductive phase. In contrast to WAXD, which exhibits lines and crystalline grains only for the low temperature crystalline phases, SAXS shows the existence of nano-grains in both the low and high temperature phases; and the average grain size changes at the phase transition temperature. The nature of the nano-grains as seen by SAXS is not just the pure crystalline but also the partly amorphous form, while WAXD records only pure crystalline nano-grains. Thus, the highly conductive phase consists of a completely amorphous polymer matrix, which, as is known, favours ion-conduction due to elastic movements of PEO chains. Furthermore, amorphous nano-grains consisting of both PEO/ZnCl₂ and ZnCl₂ structures could also contribute to Zn²⁺-ion conduction by a hopping mechanism. Under proper circumstances, the presence of ion-transport pathways can be as important as polymer segmental motion [22–24]. The irradiated polymer electrolyte has, besides higher conductivity [4], a lower phase transition temperature (54 °C) than (PEO)₈ZnCl₂ (65 °C) [25] and the nanocomposite polymer (PEO)₈ZnCl₂/TiO₂ electrolyte (71 °C) [26].

4 Conclusions

The simultaneous SAXS/WAXD/DSC measurements have shown that the nanostructure of the γ -irradiated polymer electrolyte (PEO)₈ZnCl₂ changes during the crystalline-amorphous phase transition into a highly conductive superionic phase. The conductivity is higher and the phase transition temperature lower than for non-irradiated (PEO)₈ZnCl₂, which is a desirable property for application in batteries. The significant role that the nano-dimensions of the electrolyte material play in the Zn²⁺-ion mobility was discussed. The combined SAXS/WAXD information about the evolution of the average grain sizes during the phase transition gave insight into the nano-morphology, which influences the ionic transport in a nanocomposite polymer electrolyte. Further optimizations of the electrolyte properties are in progress since these nano-structured materials are very attractive for batteries or other types of electronic devices.

Acknowledgments The Ministry of Education, Science and Sport of the Republic of Croatia is thanked for supporting this work.

References

1. S.Z.D. Chang, *Nature* **448**, 1006 (2007)
2. T.M.A. Abrantes, L.J. Alcacer, C.A.C. Sequeira, *Solid State Ionics* **18**(19), 315 (1986)
3. M.J.C. Plancha, C.M. Rangel, C.A.C. Sequeira, *Solid State Ionics* **116**, 293 (1999)
4. A. Turković, M. Pavlović, P. Dubček, M. Lučić-Lavčević, B. Etlinger, S. Bernstorff, *J. Electrochem. Soc.* **154**(6), A554 (2007)
5. S.J. Visco, M. Liu, L.C. Dejonge, Cell for making secondary batteries, Patent number 5162175, 10 Nov 1992
6. F. Brochu, M. Duval, Additives for extruding polymer electrolytes, Patent number 5622792, 22 Apr 1997
7. H. Amenitsch, S. Bernstorff, P. Laggner, *Rev. Sci. Instr.* **66**, 1624 (1995)
8. M. Ollivon, G. Keller, C. Bourgaux, D. Kalnin, P. Lesieur, *J. Therm. Anal. Calorim.* **85**(1), 219 (2006)
9. O.Glatter, O. Kratky, (eds.), *Small Angle X-ray Scattering* (Academic press, London, 1982), p. 18
10. A. Guinier, *Ann. Phys. Paris* **12**, 161 (1939)
11. G. Porod, *Kolloid-Zeitschrift* **124**, 83 (1951)
12. G. Porod, *Kolloid-Zeitschrift* **125**, 51 (1952)
13. G. Porod, *Kolloid-Zeitschrift* **125**, 109 (1952)
14. J. Baldrian, M. Horky, A. Sikora, M. Steinhart, P. Vleek, H. Amenitsch and S. Bernstorff, Annual Report 2000 Austrian SAXS Beamline at ELETTRA, 72 (2000)
15. J. Baldrian, M. Steinhart, A. Sikora, H. Amenitsch, S. Bernstorff, *Fibres and Textiles* **13**(5), 35 (2005)
16. S.Z.D. Cheng, A. Zhang, J.S. Barkley, J. Chen, *Macromolecules* **24**, 3937 (1991)
17. J. Baldrian, M. Horky, A. Sikora, M. Steinhart, P. Vleek, H. Amenitsch, S. Bernstorff, *Polymer* **40**, 439 (1999)
18. A. Turković, K. Radmanović, I. Pucić, Z. Crnjak Orel, *Strojarstvo* **44**(3–6), 203 (2002)
19. I. Pucić, A. Turković, *Solid State Ionics* **176**, 1797 (2005)
20. I.Pucić, T. Jurkin and A.Turković, Book of Abstracts, 7th Austrian Polymer Meeting (Graz, Austria, April 4–6, 2005) p. 65
21. A. Turković, P. Dubček, K. Juraić, A. Drašner, S. Bernstorff, *Materials* **3**(11), 4979–4993 (2010)
22. P. Grey, G. Greenbaum, *MRS Bull.* **27**(8), 613 (2002)
23. P.G. Bruce, *Dalton. Trans.* **11**, 1365 (2006)
24. E. Staunton, A.M. Cristie, I. Martin-Luis, Y.G. Andreev, A.M.Z. Slawin, P.G. Bruce, Agnew. Chem., Int. Ed. **43**(16), 2103 (2004)
25. A. Turković, M. Pavlović, P. Dubček, S. Bernstorff, *Acta Chim. Slov.* **55**(4), 822 (2008)
26. A. Turković, M. Rakić, P. Dubček, M. Lučić-Lavčević, S. Bernstorff, *Vacuum* **84**(1), 68 (2008)